SOUND FIELDS IN ROOMS: AN INTRODUCTION TO REVERBERATION THEORY

Jean-Dominique Polack
Laboratoire d'Acoustique Musicale
Universite Paris VI/C.N.R.S./Ministere de la Culture

0. Introduction

Since W. C. Sabine founded Room Acoustics 100 years ago, numerous authors have proposed different approaches to the characterization of sound fields in rooms. These approaches vary from purely energetic analysis, only interested in the total energy balance in a room, to more complex analysis which aim at describing the sound field at any position in the room. In the past few decades, the increasing power of computers has make

it possible to envisage full computation of a sound field in a room, but it still remains beyond our reach in the case of big rooms, such as concert halls or theatres. Therefore, a survey of the different theoretical descriptions of sound fields in rooms is necessary at the beginning of a symposium devoted to advanced research into concert halls and auditoria.

In the first Section, the different approaches to room acoustics are presented, sketching the procedures and the main results. The second Section is devoted to recent achievements in reverberation theory.

1. The theories of room acoustics

1.1 Modal analysis

Historically, modal analysis was the first attempt to derive Sabine's reverberation theory from the wave equation. It was introduced by Van Den Dungen (1934), but its definitive formulation was given by Morse & Bolt (1944). It can be found in several textbooks (Morse & Ingard 1968, Cremer et al. 1982, Bruneau 1983), so we just recall the main results.

1.1.1 General formulation

Sound fields in room can be described in both frequency and time domain. In both cases, the room is ascribed a volume (V), bounded by a wall (S) and containing a source Q (or q), as shown in Figure 1. The sound field is then the solution of a differential equation within the
volume, with boundary conditions on the surface of the wall. In the time domain, initial conditions must also be given. In the following, capital letters are reserved to the frequency

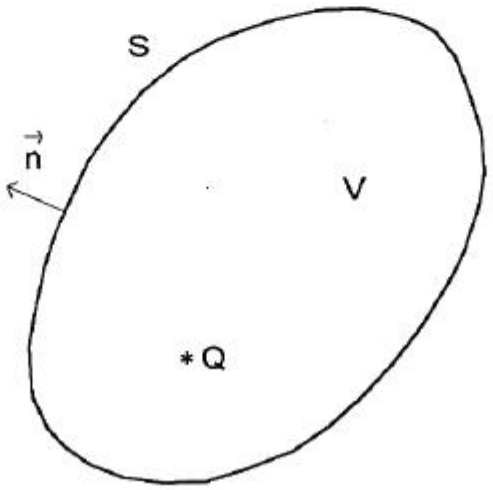

Figure 1. Geometry of the problem

domain, the spatial coordinates are defined as $\vec{r}$, frequency by $\omega=2\pi f$, and time by t. Ψ and ψ are the frequency and time solutions respectively:

frequency domain		time domain	
$\Delta\Psi + k^2\Psi = -Q(\vec{r},\omega)$	in (V)	$\Delta\psi(r,t) - c^2\partial_{tt}^2\psi(r,t) = -q(r,t)$	(1)
$\partial_n\Psi + ik\beta(\vec{r},\omega) = 0$	on (S)	$\partial_n\psi(r,t) + c^{-1}\beta(r,t).\partial_t\psi(r,t) = 0$	(2)
	initial conditions	$lim_{t\to-\infty}\psi(r,t) = lim_{t\to-\infty}\partial_t\psi(r,t) = 0$	(3)

where c is the speed of sound, $k=\omega/c$ the wave number, and β the specific admittance of the wall.

The frequency solution can be decomposed on an orthogonal basis of eigenvectors, the eigenmodes Ψ_n, giving the following expression for pressure:

$$p(\vec{r},\omega) = i\omega\rho\Psi(r) = i\omega\rho\sum_{n=0}^{\infty}\frac{\iiint_V Q(\vec{r}_o,\omega)\Psi_n(\vec{r}_o,\omega)d\vec{r}_o}{V\Lambda_n(\omega)\left[k_n^2(\omega)-\frac{\omega^2}{c^2}\right]}\Psi_n(\vec{r},\omega) \qquad (4)$$

where ρ is the mean density, and where $\Psi_n(\vec{r},\omega)$ is the eigenvector corresponding to the eigenvalue $k_n^2(\omega)$ of equations (1) and (2), normalised by:

$$\iiint_V \Psi_m\Psi_n\,dV = V\Lambda_m(\omega)\delta_{mn} \qquad (5)$$

The time solution is then given by the Fourier transform of the frequency solution:

$$p(\vec{r},t) = \frac{1}{2\pi}\int_{-\infty}^{+\infty} i\omega\rho\sum_{n=0}^{\infty}\frac{\iiint_V Q(\vec{r}_o,\omega)\Psi_n(\vec{r}_o,\omega)d\vec{r}_o}{V\Lambda_n(\omega)\left[k_n^2(\omega)-\frac{\omega^2}{c^2}\right]}\Psi_n(\vec{r},\omega)e^{i\omega t}\,d\omega \qquad (6)$$

1.1.2 Point like source

For a point like source, expressions (4) and (6) can be further developed. The frequency solution leads to the steady state regime associated to the source $Q(\vec{r},\omega) = Q_\omega\,\delta(\vec{r}_0 - \vec{r}_S)$:

$$p(\vec{r},\omega) = i\omega\rho Q_\omega \sum_{n=0}^{\infty} \frac{\Psi_n(\vec{r}_S,\omega)\vec{r}_o}{V\Lambda_n(\omega)\left[k_n^2(\omega)-k^2\right]} \Psi_n(\vec{r},\omega) \qquad (7)$$

The pressure is maximum at the poles $\omega = \omega_n + i\gamma_n$, solutions of:

$$k_n^2(\omega_n + i\gamma_n) = (\omega_n + i\gamma_n)^2 / c^2 \qquad (8)$$

As γ_n is small compared to ω_n, we obtain to the first order in γ_n :

$$k_n(\omega_n + i\gamma_n) \approx k_n(\omega_n) + i\gamma_n k_n'(\omega_n) \qquad (9)$$

similar to:

$$k_n(\omega_n + \varepsilon) = k_n(\omega_n) + c\, k_n'(\omega_n) \qquad (10)$$

Combining equations (9) and (10), we can approximate each pole by:

$$c^2 k_n^2(\omega_n + \varepsilon) - (\omega_n + c)^2 = -2\omega_n(c - i\gamma_n)\left[1 - ck_n'(\omega_n)\right] \qquad (11)$$

leading to a maximum at ε=0, and to a resonance width of $2\gamma_n$ (Figure 2).

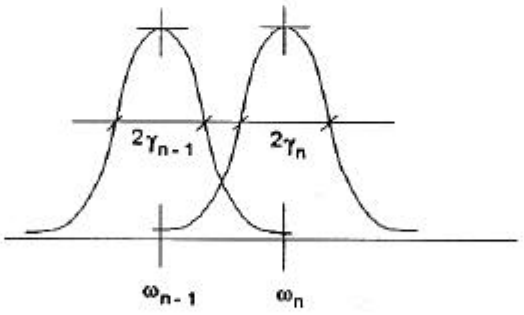

Figure 2: The eigenmodes of the steady state regime

The time solution for a continuous source turned off at time t=0
$[q(\vec{r},t) = \delta(\vec{r}_0 - \vec{r}_S)\sin\omega_g t,\ t \le 0; q(\vec{r},t) = 0, t \ge 0]$ gives the transient regime. The integration on ω can be carried out by the residu technique (Morse & Ingard 1968), leading to:

$$p(\vec{r},t) = \begin{cases} \rho c^2 \omega_g \sum B_n \cos(\omega_g t + \Gamma_n) & t < 0 \\ \rho c^2 \omega_g \sum_n^n C_n e^{-\gamma_n t} \cos(\omega_g t + \Omega_n) & t > 0 \end{cases} \qquad (12)$$

where $B_n\exp\{i\Gamma_n\}$ and $C_n\exp\{i\Omega_n\}$ are complex coefficients given by the values taken by the eigenfunctions $\Psi_n(\vec{r},\omega)$ at positions $\vec{r}$ and $\vec{r}_S$ and at frequencies ω_g ($t<0$) and $\omega_n+i\gamma_n$ ($t>0$). $\omega_n+i\gamma_n$ are the poles defined by equation (8). Equation (12) plainly shows that each pressure mode decays exponentially after the source has been turned off.

1.2.3 Approximate solutions

In practice, expressions (7) and (12) are inextricable, even if only one mode is considered. Further, the existence of eigenmodes cannot be proved mathematically as soon as the wall admittance β has a non vanishing real part, that is, as soon as walls are absorbing. Morse & Ingard (1968) therefore proposed a two step perturbation method.

The first step consists in computing the eigenvalues of a slightly different room for which mathematical theorems prove the existence of eigenfunctions: typically, a room (V_0) with hard walls (S_0), depicted in Figure 3. The eigenvalues of the new rooms are thus given by:

$$(\Delta + n_n^2)\Psi_n^0 = 0 \qquad \text{in } V_0 \qquad (13)$$

$$\partial_n \Psi_n^0 = 0 \qquad \text{on } V_0 \qquad (14)$$

The eigenvalues build up an orthogonal basis normalised by:

$$\iiint_{V_0} \Psi_n^0 \Psi_m^0 \, dV = V_0 \Lambda_n^0 \delta_{mn} \approx \iiint_V \Psi_n^0 \Psi_m^0 \, dV \qquad (15)$$

to the first order. Applying Green's theorem in the original volume (V) to the original solution $\Psi(\vec{r})$ and to the new eigenvalues, and letting $\Psi(\vec{r})$ tend toward Ψ_n, that is, k^2 toward k_n^2 and Q(r) toward 0, leads to an expression of the original eigenvalues to the second order in Ψ_n^0:

$$k_n^2(\omega) = n_n^2 + \frac{1}{V_0 \Lambda_n^0} \iint_S \Psi_n^0 \left[ik\beta + \partial_n\right] \Psi_n^0 dS = \eta_n^2 + 2\eta_n < ik\beta + \partial_n > \qquad (16)$$

where notation <a> corresponds to the surface integral dS

$$\frac{1}{2n_n V_0 \Lambda_n^0} \iint_S \Psi_n^0 \, a \, \Psi_n^0 dS$$

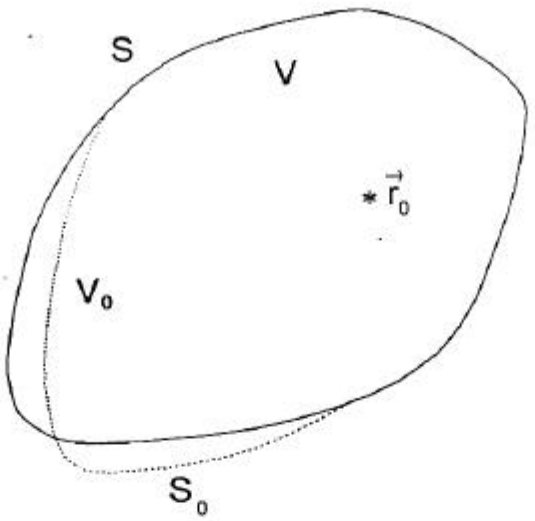

Figure 3: The geometry of the perturbated problem

Writing $\beta(\vec{r},\omega) = \xi(\vec{r},\omega) + i\sigma(\vec{r},\omega)$, and setting in the surface integral $k=k_n=\omega_n+i\gamma_n$ we can separate the real and imaginary parts of the poles:

$$\frac{\omega_n}{c} = \eta_n + < -\eta_n\ \sigma(\eta_n) + \partial_n > \qquad \frac{\gamma_n}{c} = < \eta_n\ \xi(\eta_n) > \tag{17}$$

Since γ_n is linked to the decay rate of the mode after the source is turned off (see equation 12), this decay rate is in first approximation proportional to the mean value taken by the real part ξ of the specific admittance β on the wall:

$$\gamma_n = \frac{cS\Lambda_n}{2V_0\Lambda_n^0}\bar{\xi} \qquad S\,\Lambda_n^S \approx \iint_S \Psi_n^0\ \Psi_n^0\ dS \tag{18}$$

Therefore the real part of the admittance must be positive in all physically relevant cases.

In a second step, the original eigenvalues are also approximated. These eigenvalue satisfy the following system to first order in $\Psi_n{}^0$:

$$(\Delta + k_n^2)\Psi_n = 0 \qquad \text{in V} \tag{19}$$

$$\partial_n \Psi_n = -ik\,\beta\,\Psi_n \approx -ik\,\beta\,\Psi_n^0 \qquad \text{on S} \tag{20}$$

Adapting to Ψ_n the expression (4) for $\Psi(\vec{r})$, we obtain:

$$\Psi_n(\vec{r}) = \Psi_n^0(\vec{r}) + \sum_{m\neq n} \frac{\iint_S \Psi_n^0 (ik\beta + \partial_n .)\Psi_m^0 dS}{V_0\Lambda_m^0\left[k_n^2 - n_m^2\right]}\Psi_m^0(\vec{r}) \tag{21}$$

Therefore, the wall admittance couples together the eigenmodes of the hard room, according to the integral:

$$\iint_S \Psi_n^0 (ik\beta + \partial_n .) \Psi_m^0 dS_0 \qquad m \neq n \qquad (22)$$

However, the coupling does not modify expression (16) for the original eigenvalues.

The coupling between eigenmodes introduced by a wall admittance is the major result of modal analysis. It explains how the energy contained in each mode can migrate in the adjacent modes, thus regulating the decay rate of all adjacent modes to an average value (strong coupling). The computation of this average decay rate remains nevertheless an impossible task.

1.2 Statistical analysis.

Originally, the statistical analysis of sound fields in rooms was restricted to the transfer function, that is, to the random superposition of modes. The name of Schroeder is attached to this analysis (see e.g. Schroeder 1954a, 1954b, 1969). More recently, statistical analysis of impulse responses, that is, of transient phenomena, have been available (Polack 1988, Jot 1992).

1.2.1 Eigenmode density

The following presentation is only valid in rectangular rooms, but H. Weil showed in 1911 that the result remains valid for rooms of arbitrary shapes. Only the leading term of the development in powers of the frequency is given here: the nest terms depend on the geometry of the room, as interested readers can read in Bloch & Balian (1970).

In a rectangular room, eigenfrequencies are given by:

$$\upsilon_n^2 = \left(\frac{k_n c}{2\pi}\right)^2 = \left(\frac{n_x c}{2\ell_x}\right)^2 + \left(\frac{n_y c}{2\ell_y}\right)^2 + \left(\frac{n_z c}{2\ell_z}\right)^2 \qquad (23)$$

In other words, eigenfrequencies are distributed on the nodes of a lattice, each cell of which contains an elementary "volume" of the frequency space (see Figure 4):

$$\upsilon_c \approx \frac{c}{2\ell_x} \cdot \frac{c}{2\ell_y} \cdot \frac{c}{2\ell_z} = \frac{c^3}{8V} \qquad (24)$$

where $V=\ell_x.\ell_y.\ell_z$ is the volume of the room.

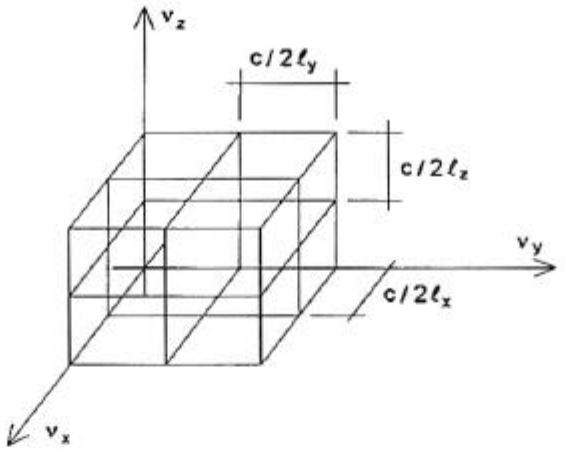

Figure 4: The lattice of eigenvalues in a rectangular room

As a consequence, the number of eigenfrequencies contained between frequencies ν and (ν+dν) are given by the number of lattice nodes contained in the portion of sphere of radius ν and thickness dν. Actually, as shown in Figure 4, the eigenfrequencies are only distributed over one eighth of the sphere, leading to the following expression for the volume of the portion of sphere:

$$\upsilon_V = \frac{4\pi\upsilon^2}{8} d\upsilon \tag{25}$$

Dividing this volume by the volume of an elementary cell gives the leading term for the distribution of eigenmodes between frequencies ν and (ν+dν) :

$$dN = \upsilon_v \,/\, \upsilon_c = \frac{4\pi V\ \upsilon^2}{c^3} d\upsilon \tag{26}$$

Thus, the number of eigenfrequencies increases, in first approximation, as the square of the frequency. This leads to separate two frequency regimes:

- at low frequencies, eigenmodes are isolated, because their density is low. Modal analysis is fully relevant, as proved by the practice of reducing low frequency resonances by modifying the wall impedance at pressure maxima (Helmholtz resonators).

- at high frequencies, many modes are overlapping. Modal analysis must be understood in a statistical manner: we enter the regime of "large rooms", or Schroeder regime, where other techniques proves more efficient in practice (see Section 1.3).

The limit between the two regimes is given by Schroeder frequency:

$$f_S = 2000\sqrt{T/V} \tag{27}$$

where T is the reverberation time which is linked to the width of the modes (see below Section 1.2.3). Expression (27) corresponds to a superposition of 3 modes within a frequency interval equal to their average width.

1.2.2 Transfert function

At high frequencies (Schroeder regime), equation (7) for the steady state field can be further developed, leading to an estimate of the mean squared pressure in the room. Firstly, the squared pressure is averaged in the whole room, taking into account the orthogonality of the eigenmodes:

$$\left\langle p_{rms}^2(\omega)\right\rangle_V = \frac{1}{2}\int_V \left|p_\omega(\vec{r})\right|^2 dV = \frac{1}{2}\left(\frac{\omega_0}{V}\right)^2 \left|Q_\omega\right|^2 \sum_n \frac{\left|\Psi_n(\vec{r}_0,\omega)\right|^2 / \Lambda_n}{\left|k_n^2 - k^2(\omega)\right|^2} \qquad (28)$$

Secondly, the summation is carried out on all eigenvalues belonging to a small frequency interval around $\omega=2\pi\nu$. These eigenvalues are given by equation (16), with the simplification that the volumes (V) and (V_0) are equal so that normal derivatives vanish on the boundary, that is:

$$k_n^2(\omega) = n_n^2 + \frac{1}{V_0\Lambda_n^0}\iint_S \Psi_n^0[ik\beta]\Psi_n^0 dS = n_n^2 - \frac{k}{4V}[g_n(\omega) - ia_n(\omega)] \qquad (29)$$

where we have introduced the quantities:

$$a_n \approx \frac{8V}{c}\gamma_n \approx 8\,\bar{\xi}\,S \qquad \text{and} \qquad g_n \approx 8V[\eta - \omega_n/c] \approx 8\,\bar{\sigma}\,S \qquad (30)$$

g_n measure the frequency shift of the eigenmode. In expression (28) for the mean squared pressure, the denominator becomes:

$$\left|k_n^2 - k^2(\omega)\right|^2 = (n_n^2 - k^2 - \frac{kg_n}{4V})^2 + (\frac{ka_n}{4V})^2 \qquad (31)$$

Since the density of eigenmodes is high at high frequencies, the summation can be replaced by an integral on eigenfrequencies weighted by their density, leading to the following expression for the mean squared pressure when the a_n are considered as constant:

$$\left\langle p_{rms}^2(\omega)\right\rangle_V = \frac{1}{2}\frac{\rho^2\omega^2}{\pi a}\left|Q_\omega\right|^2 E(\vec{r}_S) = \Pi_\omega / a \qquad (32)$$

Equation (32) was first obtained by Sabine, using energy considerations. The mean squared pressure is thus inverse proportional to a quantity representing the amount of absorbing material contained in the room. This quantity has the dimensions of a surface, as can be seen from expression (30).

Equation (32) constitutes a very important results since it shows that the mean squared pressure in a room is independent of the distribution of eigenmodes. Furthermore, Schroeder (1954) was able to show that this independency subsists for the fluctuations of the mean squared pressure, that is, for the fluctuations of the transfer function: their mean amplitude is 5.6 dB in every room. The method used by Schroeder essentially amounts to the statistical superposition of eigenmodes, that is, he assumed their phases as randomly distributed, in accordance with experiments. Using the central limit theorem, the resulting transfer function can be considered as a complex Gaussian process with a mean value equal to zero and a variance given by equation (32). Many other average quantities can be deduced from this process.

1.2.3 Reverberation

Reverberation takes place in a room when a source is suddenly turned off. The case of a monochromatic point-like source has already been analysed in Section 1.1.2 (equation 12): each eigenmode decays while oscillating at its eigenfrequency, with initial phases and amplitudes depending on the corresponding eigenfunctions.

As for the steady state regime, it is however possible to estimate the mean value taken by the squared pressure in the whole room at every moment. Due to the othogonality of eigenmodes, only quadratic terms subsist in the sum, leading to:

$$\left\langle p_{rms}^2(t)\right\rangle_V = \frac{1}{2}\sum_n |R_n|^2\, e^{-2\gamma_n t}\cos^2(\omega_n t+\Omega_n) = \frac{1}{2}\sum_n |R_n|^2\cos^2(\omega_n t+\Omega_n)\, e^{-\frac{ac}{4V}t} \qquad (33)$$

where the coefficients a_n are still given by equation-(30).

If we assume a_n and γ_n as slowly varying with frequency, the exponential term can be taken out of the sum, and the decay of the mean squared pressure becomes:

$$\left\langle p_{rms}^2(\omega)\right\rangle_V = p_0^2\, exp\left\{-\frac{ac}{4V}t\right\} \qquad (34)$$

Expression (34) was also obtained by Sabine originally. it allows the computation of the reverberation time T - the time taken by the mean squared pressure to decay by 60 dB - by means of Sabine's formula:

$$T = 0.16\frac{V}{a} \qquad (35)$$

Expression (34) relies therefore on two assumptions. First, we assumed $a_n n$ and γ_n as slowly varying with frequency, but Jot (1992) has shown, in the case of reverberation filters, that γ_n slowly varying with frequencies are essential to avoid a decay dominated by a few modes only. Therefore this assumption is likely to hold in practice, though it has never been proved. Second, we have considered the quantity $p_0 = (1/2)\sum_n R_n \cos(\omega_n t + \Omega_n)$ as constant. This approximation is only valid when the sum covers a large band of frequencies. For narrow bands of frequencies, an oscillatory behaviour subsists for p_0. This is consistent with the practice of measuring sound decay in large bands of frequencies: the octave bands. No improvement can be achieved by choosing narrow bands: reverberation essentially is a statistical process.

1.2.4 Stochastic models for impulse responses.

In fact, all the statistical properties of the transfer function (see Section 1.2.2) translate into the time domain, that is, in the impulse response: the random superposition of eigenmodes translates into a Gaussian random process, with zero mean and a variance decreasing with time according to Sabine's formula (35). Further, the mean frequency response can be recovered if the process is Markovian, that is, if a proper correlation is set between successive samples of the process. This correlation introduces a new parameter, the equivalent statistical bandwidth B of the response, defined by:

$$B = \frac{1}{2\pi}\left[\int_0^\infty |H(\omega)|^2 d\omega\right]^2 \Big/ \left[\int_0^\infty |H(\omega)|^4 d\omega\right] \qquad (36)$$

With help of this parameter, many statistical properties related to "noise" rejection - in fact the rejection of random fluctuations - can be established (see Polack 1988), such as the emergence of the initial peak of the autocorrelation function of an impulse response (35 dB in the case of Figure 5 measured in Espro at IRCAM, Paris). A similar magnitude of rejection is predicted for the modulation transfer function, that is, the Fourier transform of the squared impulse response, explaining why this function gives rise to a very robust measure of speech intelligibility: the Speech Transmission Index

However, the Gaussian model for the impulse response, even in its Markov variant, suffers from a major drawback: it cannot account for reverberation times varying with frequencies, since the correlation between samples is fixed. In order to obtain reverberation times varying with frequencies, the variance of the process must be defined by a time-frequency distribution, slowly varying with frequency and exponentially decreasing with time. Polack (1988) proposed the mean Wigner-Ville spectrum, defined as the ensemble average of the Wigner-Ville distribution:

$$\begin{aligned} W_h(t,\omega) &= \int h(t-\tau/2)\, h(t+\tau/2)\, e^{-j\omega\tau} d\tau \\ &= (1/2\pi) \int H^*(\omega-\Omega/2)\, H(\omega+\Omega/2)\, e^{j\Omega t}\, d\Omega = W_H(t,\omega) \end{aligned} \qquad (37)$$

which is directly linked to the mean time and frequency quadratic responses:

$$(1/2\pi)\int W_h(t,\omega)\,d\omega = h^2(t) \quad ; \quad \int W_h(t,\omega)\,dt = |H(\omega)|^2 \tag{38}$$

Note that a Wigner-Ville distribution can take negative value, hence the necessity of using the WignerVille spectrum.

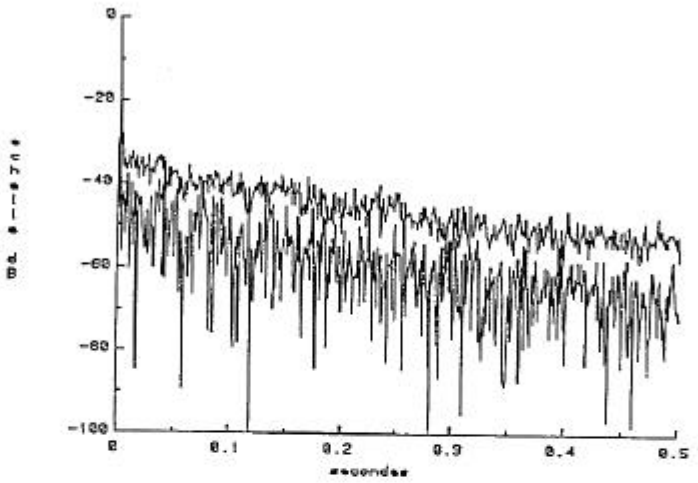

Figure 5: Autocorrelation function measured in ESPRO
upper curve: mean squared
lower curve: mean value

In his seminal thesis on reverberation filters, Jot (1992) replaces the Wigner-Ville spectrum by the future running spectrum of Page-Levin, defined by:

$$P_h^+(t,f) = -\frac{\partial}{\partial t}\left|\int_t^{+\infty} h(\tau)e^{-j2\pi f\tau}\,d\tau\right|^2 \tag{39}$$

which generalises Schroeder's reverse integration since:

$$\int_{t=\tau}^{+\infty} P_h^+(t,f)\,dt = \left|\int_{t=\tau}^{+\infty} h(t)e^{-j2\pi ft}\,dt\right|^2 \tag{40}$$

Besides, the future running spectrum still satisfies relations (38) and only takes positive values. Jot's analysis of existing rooms with this distribution shows that above Schroeder frequency (equation 27), smooth "energy decay reliefs" can be calculated from reverse integration of the future running spectrum by estimation of the reverberation time of each narrow frequency band (Figure 6).

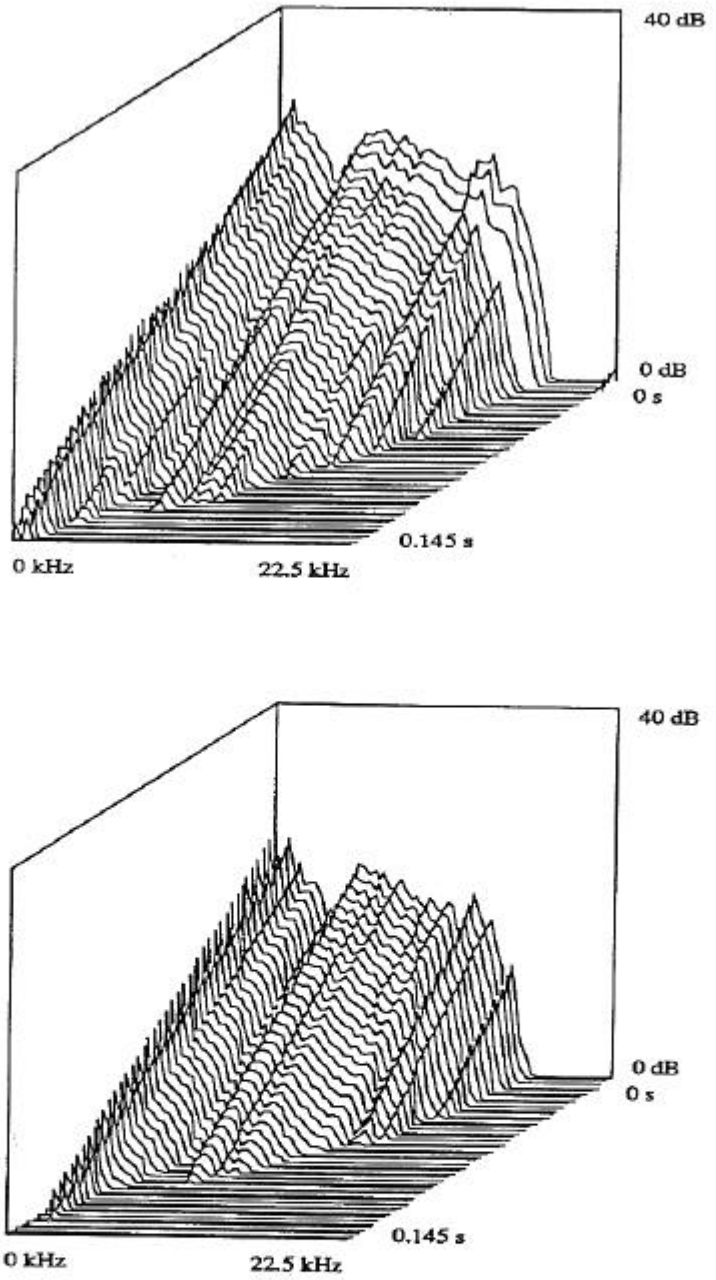

Figure 6: Energy decay reliefs in a studio
above: measured with the future running spectrum
below: smoothed by reverberation estimation (from Jot 1992)

1.2.5 Distribution of arrivals

The stochastic models presented in Section 1.2.2 suffers one major drawback: it is only valid if many pulses, or arrivals, are sent back to the receiver simultaneously by the room.

Bolt et al. (1950) have studied the density of arrivals in a rectangular room. This density can easily be deduced from tiling the Euclidian space with all the images of the room

obtained by mirroring it on its walls (Figure 7), and from the corresponding image sources. Each arrival reaching the receiver between times t and (t+dt) originates therefore from one of the image sources located between the spheres of radius ct and c(t+dt) centred on the receiver position. The same procedure as in Section 1.2.1 for the modal density can be used since each image of the room only contains one single image source, leading to a density of arrivals equal to the ratio of the volume of the portion of sphere ct and thickness c.dt to the volume (V) of the room, that is:

$$dN(t) = \frac{4\pi c^3 t^2}{V} dt \qquad (41)$$

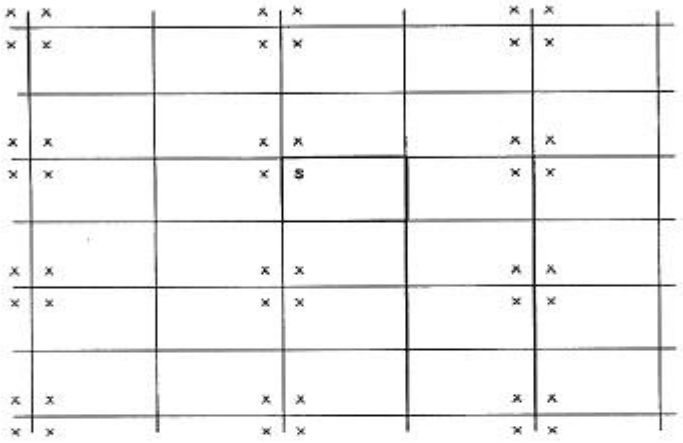

Figure 7: Tiling the Euclidian space
(S: source; X: image sources)

In order to approximate the impulse response with a Gaussian process, at least 10 arrivals must fall within the observation time. According to the size of the observation time, the mixing time, defined here as the time after which a minimum of 10 arrivals always fall on the receiver during the observation time, can differ. Thus, for Espro at IRCAM, Paris, a rectangular room of 3545 m^3 in the usual configuration, the mixing time is:

1.5 s for 33 μs observation time (sample time in Figure 8a)
270 ms for 1 ms observation time (sample time in Figure 8b)
55 ms for 24 ms observation time.

The last observation time correspond to the time constant of the human hearing and bear no connection with Figure 8. However, the corresponding mixing time agrees well with visual estimation on Figure 8: tiling the Euclidian space with the images of the room leads to an underestimation of the mixing time.

In fact, exact tiling of the Euclidian space does not happen for every room. In general, the image sources obtained by permutations of the reflecting surfaces do not coincide, and the number of image sources grows exponentially. However, most of the image sources are hidden behind some walls for any receiver position. As will be explained in Section 1.3,

hidden image sources are usually discarded, which amounts to discarding diffracted rays. The question remains open whether hidden sources should be kept or not, and in the affirmative, how to account for them.

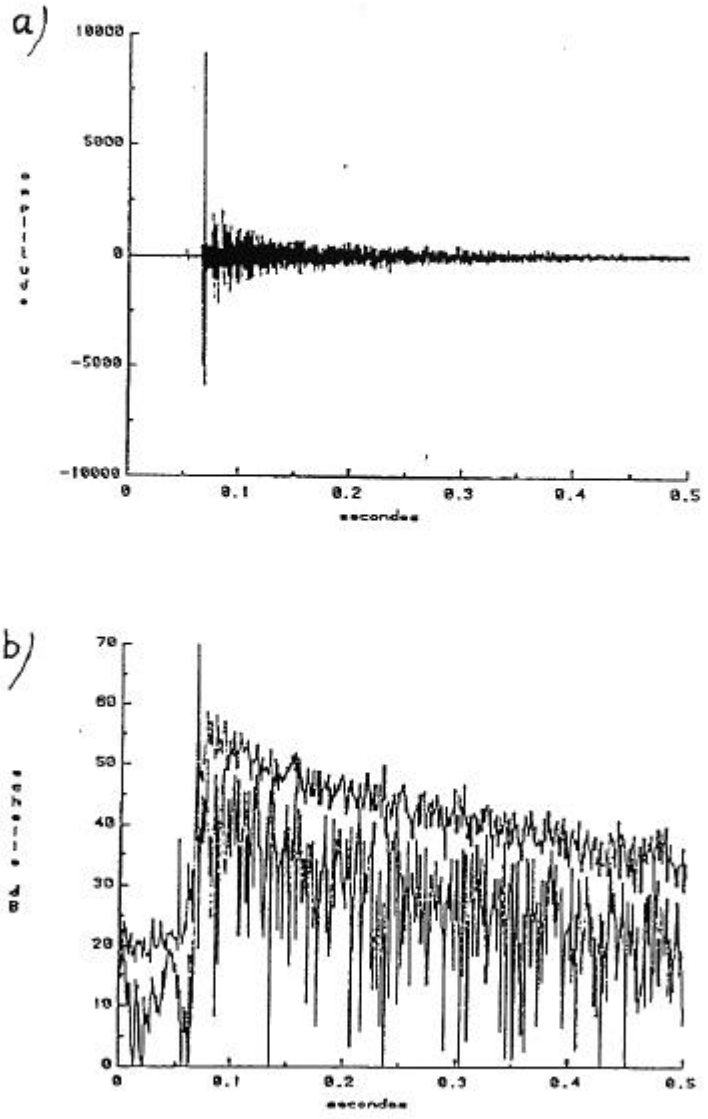

Figure 8: Impulse response measured in ESPRO
a) raw response
b) mean squared (above) and mean (below)

1.3. The geometrical approach.

Of all the approaches to room acoustics, geometrical acoustics is certainly the most intuitive and the oldest one. It rests on the analogy between acoustics and optics, and remains the main techniques used for computer simulation of room acoustics.

1.3.1. Geometrical acoustics

By analogy with geometrical optics, geometrical acoustics assumes that sound propagates along lines called sound rays. However, unlike optics, the wave properties of sound can never be neglected: to a greater extent than in optics, geometrical acoustics therefore considers the propagation of wave fronts, which usually are equiphase surfaces, along the rays. These rays must satisfy Fermat principle, that is, the acoustical path linking two points always is an extremum.

Geometrical acoustics proves particularly useful at high frequencies where wavelengths are small in comparison with room dimensions. Geometrical acoustics can therefore be viewed as a complement to modal analysis, ill-adapted to high frequencies where mode superposition leads to statistical fields (Section 1.2). In fact, this complementarity is fundamental: wave fronts and rays can be directly deduced from the wave equation by means of Hadamard's characteristics theory (see e.g. Courant & Hilbert 1962). There is therefore total equivalence between geometrical and wave acoustics.

In the general case, rays satisfy nonlinear equations that must be solved numerically (see Pierce 1981). In room however, where air is an homogeneous isotropic medium, these equations are greatly simplified, and rays reduces to straight lines perpendicular to wave fronts. The latter propagate at constant speed - the speed of sound - along the rays.

This simplified description is considered in most applications: a wave front is followed as it propagates inside a room and undergoes multiple reflections on the walls. This propagation can be assimilated to the uniform rectilinear mouvement of a point - a sound-particle, or phonon - in the room (Polack 1992). This mouvement has received considerable attention from mathematicians because it constitutes one of the simplest examples of dynamical systems: billiards. Billiards display many interesting statistical properties, including chaos.

1.3.2 Sound intensity.

At its elementary level, geometrical acoustics only traces rays in the room, assuming specular reflections on the walls. In the old days, rays were traced on plans and sections of the room, but elaborate three-dimensional computer programs have been recently developed (Epidaure, Odeon, etc.) that make it possible to predict acoustical parameters at design stage.

The variation of sound energy along a ray can also be computed by considering a tube of rays instead of one single ray. During propagation, the cross-section of the tube varies: it can be shown from the wave equation that sound intensity along the tube is inverse proportional to the cross-section. Taking also into account phases, given by a combination of tube lengths and frequencies, the acoustical pressure can even be computed everywhere in the room and the whole sound field reconstituted. This last step is not implemented in actual programs because of the enormous computing resources it demands.

1.3.3 Caustics

At some spatial positions, the cross-section of a ray tube may vanish, leading to diverging sound intensity. Such position are located in the vicinity of sound field singularities, called caustics or focal lines. More precisely, caustics are envelopes of ray bundles crossing on its vicinity (Figure 9). Caustics constitute therefore so-called "optical" boundaries separating an "illuminated" zone from a "shadow" zone. In shadow zones, geometrical acoustics cannot account for the sound field. It must be extended into the Geometrical Theory of Diffraction (GTD, see e.g. Pierce 1981), and even in the Uniform Theory of Diffraction on the caustic itself (an asymptotic expansion of the intensity in the vicinity of singularities, see Ludwig 1966).

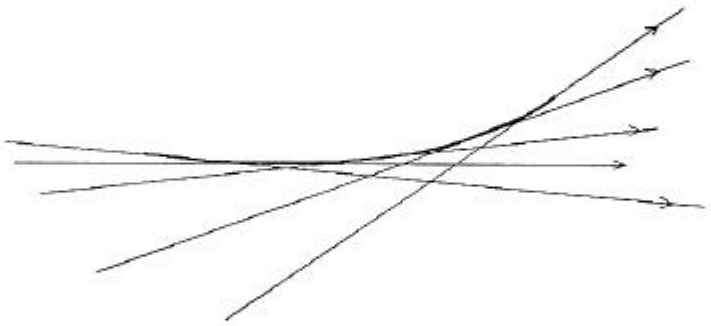

Figure 9. Rays and caustic (bold line)

As regard wave fronts, they also display singularities on caustics (reversion points). Alternatively, this singularity can be viewed as a phase shift of $\pm\pi/2$ where the ray grazes the

caustic: passing through a caustic corresponds to a spatial Hilbert transform. Very recently, Mortessagne (1994), in his seminal thesis on the semiclassical approximation in room acoustics, has been able to include caustics in geometrical acoustics, thus obtaining very accurate impulse responses (Figure 10).

1.3.4 Image sources

Instead of considering rays or ray tubes emitted by the source with specular reflections on the walls of the room, the images of the source through multiple reflections on the wall can be considered together with all the rays linking these images to the receiver. Due so

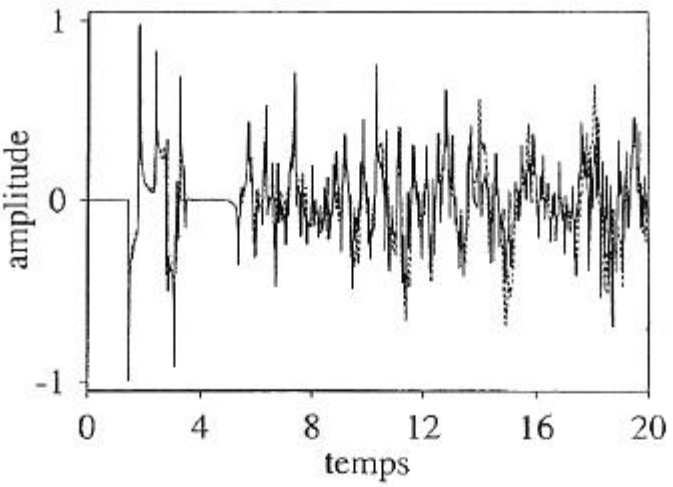

Figure 10: Semiclassical approximation of an impulse response (original in dotted lines; from Mortessagne 1994)

successive reflections, the number of images grows very quickly, in fact, exponentially, but most images are "hidden" for the receiver. However, hidden images emit diffracted rays in direction of the receiver, and the Geometrical Theory of Diffraction allows to evaluate the intensity carried out by these diffracted rays: it fades out very quickly, in fact exponentially. As a consequence, diffracted rays are neglected in most applications without checking whether their large number do not compensate for their fading . Note that the rays linking image sources to the receiver precisely give rise to the arrivals analysed in Section 1.2.5, thus stressing the role played by diffracted rays to increase the arrival density. The semiclassical approximation (Mortessagne 1994) is also constructed upon these rays, but cannot be use at its present stage to either validate or refute the discarding of diffracted rays.

1.3.5 Statistical properties

The geometrical approach also admits a statistical analysis within the frame of billiard theory. In Section 1.3.1, we mentioned that billiards constitute one of the simplest examples of dynamical systems. The statistical analysis of billiards is postponed until Section 2 where it will be used as the foundation of recent advances in reverberation theory.

1.4. Energy analysis

Rebuffed by the complexity of the preceding analysis, many acousticians turned to more phenomenological approaches based on energy balance. Historically, energy balance was first considered by Sabine 100 years ago when he studied the phenomenon he called reverberation, turning him into the founder of modern room acoustics.

1.4.1 The synthetic theory of reverberation

Introduced by Bosquet (1967), this theory constitutes the framework of any energy analysis of room acoustics. It simply consists in applying Noether theorem to the wave equation, hence obtaining the energy balance anywhere in the room.

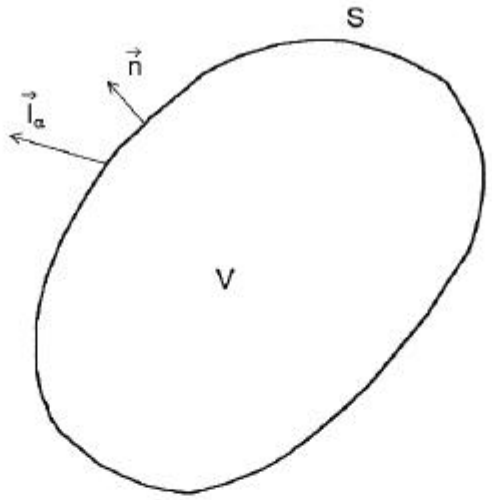

Figure 11: The geometry of Noether theorem

Multiplying by $\partial_t \psi(\vec{r},t)$ the wave equation (1) in (V) - see Figure 11 - and using product rules for derivation we obtain the local energy balance:

$$\partial_t \left\{ \frac{1}{2} \left| \frac{\partial_t \Psi}{c} \right|^2 + \frac{1}{2} \left| \vec{\nabla} \Psi \right|^2 \right\} - \vec{\nabla} . \left\{ \partial_t \Psi . \vec{\nabla} \Psi \right\} = \left\{ q \, \partial_t \Psi \right\} \qquad (42)$$

which can also be written with the help of the instantaneous sound energy density wt, the sound intensity vector $\vec{I}$. and the work π of the sound sources:

$$\partial_t w_t - \vec{\nabla} . \vec{I} = \Pi(\vec{r}_S, t) \qquad (43)$$

Integrating the local energy balance over the whole volume (V) of the room leads to the total energy balance in the room:

$$\partial_t \int_V w_t dV - \int_S \vec{I} . \vec{n} dS = \Pi(t) \qquad (44)$$

where Π is the total work of the sources, and $\vec{I}_a$ the sound intensity leaving the room through the walls (S), that is, the sound intensity absorbed by the walls. This absorbed intensity can be linked to the intensity $\vec{I}_t$ incident on the wall by introducing the absorption coefficient α and its mean value $\overline{\alpha}$ on the wall:

$$\vec{I}_a = \alpha \vec{I}_S \quad ; \qquad V \partial_t w_m(t) - \overline{\alpha} \int_S \vec{n}.\vec{I}_a \, dS = \Pi \tag{45}$$

where we also introduced the mean instantaneous energy density $w_m(t)$.

Within the frame of the synthetic theory of reverberation, evaluating the energy balance reduces to the following problem: find the relation linking sound intensity I and instantaneous sound energy density w_t everywhere in the room. By analogy with fluid mechanics, we call behaviour law any such relation, whereas the energy balance is a conservation law. As in fluid mechanics, behaviour laws are approximations deduced from phenomenological considerations, the most commons of which are now reviewed.

1.4.2 The diffuse field approximation

The so-called diffuse field approximation can be traced back to Sabine's first work on room acoustics. It rests on two assumptions:

* the instantaneous sound energy density takes the same value in the whole room;

* the sound intensity vector has the same magnitude in every directions.

With these two assumptions, intensity and energy density can be linked together by means of the following behaviour law:

$$\left|\vec{I}\right| = \frac{w}{4\pi}.c \quad , \qquad \text{where} \quad w = w_m(t) \tag{46}$$

In particular, on the wall (S) of the room, we obtain:

$$\int_S \vec{I}_a.\vec{n}\, dS = \frac{w}{4} c S \tag{47}$$

that is, on the wall, only every fourth direction points toward the wall, corresponding to a solid angle of π steradian. The total energy balance becomes:

$$\partial_t w - \frac{\overline{\alpha} S c}{4V} w = \frac{\Pi}{V} \tag{48}$$

Using instead the quantity of absorbant $a = \overline{\alpha} S$, the total energy balance leads to expression (32) obtained in Section 1.2.2 by statistical analysis of the steady state regime, provided that sound energy is considered as evenly distributed between potential and kinetic energies (i.e., $\langle p^2_{rms} \rangle = w/2$). In a similar fashion, integrating the total energy

balance directly leads to the exponential decay of the reverberation field after the source has been turned off:

$$w(t) = w_0 \exp\left\{ -\frac{a\,c}{4V} t \right\} \qquad (49)$$

an expression similar to expression (34) of Section 1.2.3; and therefore also leads to Sabine's formula (35) for the reverberation time.

Thus, the diffuse field approximation leads to simple expressions for both steady state and transient regimes. This explains why it is so widely used and abused (see Vér 1978), even when its two assumptions are blatantly breached. In fact, the diffuse field approximation is only valid at low absorptions, since a simple argumentation shows its assumptions to be incompatible with any absorption. In the presence of absorption, the total energy balance (44) stipulates that the sound intensity flow be non vanishing on the absorbing wall: some energy therefore "migrates" from the source to the walls. As a consequence, the sound intensity vector, which locally describes this migration at all positions in the room, cannot vanish on average as predicted by the uniform distribution of intensity in all directions: the second assumption of diffuse sound fields obviously is erroneous .

1.4.3 Propagation

Aware of the limitations of the diffuse field approximation, many acousticians have tried to improve the behaviour law. Almost all these trials rest on the geometrical approach: sound fields are built up by many rays which carry all the sound energy in their directions of propagation. The behaviour law then takes the very simple form:

$$\vec{I} = w\,\vec{c} \qquad (50)$$

where c is the speed of sound oriented in the direction of ray propagation.

In Section 1.2.5, we defined a mixing time as the time after which the impulse response can be described by a random process. Anticipating on Section 2, the mixing time can alternatively be defined as the time after which we no longer know the position or the direction of any ray issued from the source. The quantity of energy absorbed by the walls at the following instant is proportional to the energy flow incident on the wall, to which only contributes the impinging rays, that is, the rays located in a thin layer around the wall and properly directed. As in kinetic gas theory for evaluating the static pressure, the probability to obtain one more reflexion during the next lapse dt is:

$$\frac{S\,c}{4V}\,dt \qquad (51)$$

Two further assumptions lead to Sabine's energy balance: the uniform distribution of energy in the whole room, so that the energy carried by all the rays be the same at any given time; and above all, an instant mixing time, meaning that at the next instant, we do not know where is the ray, so that the probability of reflexion still is given by equation (51).

In fact, if the mixing be instant and all rays carry the same energy, the energy takes on average a constant value in the room at any given time. The assumption of instant mixing, obviously erroneous as shown in Figure 8, is therefore the central assumption of the diffuse field approximation.

1.4.4 Wall diffusion

If rays are propagating along straight lines and if the behaviour law is given by equation (50) along each ray, how can a diffuse sound field be obtained ? This question seems paradoxical. but only because the role played by the walls is underestimated: diffusion in a room is created by its walls. As a consequence, many authors proposed to reject the assumption of specular reflection on the walls and replace it by a "diffuse" reflection law: Lambert law. Lambert law stipulates that the reflection angle of a ray on a wall is independent on the incidence angle and is distributed on the whole half space, and that the sound intensity of the reflected ray is proportional to the solid angle at which the moving point sees the wall (Figure 12):

$$\vec{I} = B_0 \frac{\cos\theta}{\pi r^2} dS \qquad (52)$$

where $(\cos\theta/r^2)dS=d\Omega$ measures the solid angle at distance r from the wall for the slope θ of the ray, and where $B_0dS=I_0\cos\theta_0 dS$ is the instantaneous incident energy flow on the wall. In other words, each sound-particle can follow several paths after reflection, which is incompatible with dynamical systems as will be seen in Section 2. Lambert law is therefore exclusive of the most recent developments in reverberation theory.

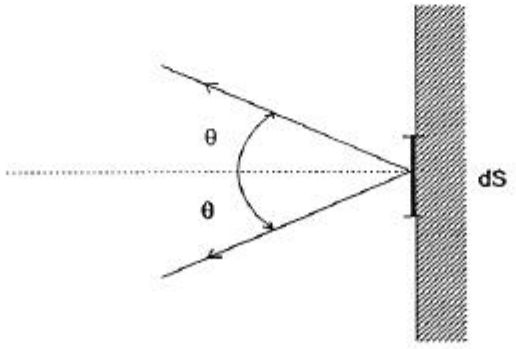

Figure 12: Lambert law

Lambert law reduces the energy balance to a surface integral. At each instant, the surface element dS' (see Figure 13) receive a flow $B(\vec{r}')dS'$and emit in the whole half-space the

flow $B(\vec{r}')[1-\alpha(\vec{r}')]$ where α is the absorption coefficient on the wall. The portion of this flow emitted in each direction is given by Lambert law, that is, for the surface element dS of Figure 13:

$$dI(R,\theta) = B(\vec{r}')\left[1-\alpha(\vec{r}')\right]\frac{\cos\theta'}{\pi R^2}\,dS' \tag{53}$$

Summing the contributions from all the surface elements, the total instantaneous flow received by element dS becomes:

$$\mathcal{B}\,dS = \iint_S \cos\theta.dI(R,\theta)dS = \frac{dS}{\pi}\iint_S\left[1-\alpha(\vec{r}')\right]B(\vec{r}')\cos\theta.\frac{\cos\theta\,dS'}{R^2} \tag{54}$$

and we obtain Kuttruffls equation:

$$\mathcal{B}(\vec{r}) = \frac{1}{\pi}\iint_S\left[1-\alpha(\vec{r}')\right]B(\vec{r}')\cos\theta.d\Omega' \tag{55}$$

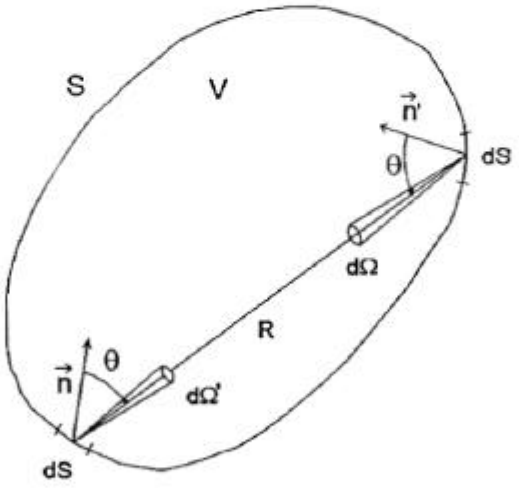

Figure 13: The geometry of Kuttruff's equation

Kuttruff's equation is defined in the time domain. It take into account the flight times between the different wall elements. Together with the behaviour law $\vec{I} = w\vec{c}$ it allows the calculation of the sound energy density at all times throughout the room. When restricted to the reverberation field, it can be further simplified by the assumption that the spatial energy distribution does not change during reverberation, but only its level. This assumption is perfectly compatible with the total energy balance (44). Therefore, the flow received at each instant by each surface element is a fraction, uniform on the whole surface, of the flow received at the previous instant. Setting $\mathcal{B}(\vec{r}) = \lambda B(\vec{r})$ with $\lambda<1$, we obtain an integral eigenvalue equation:

$$\lambda B(\vec{r}) = \frac{1}{\pi}\iint_S \left[1-\alpha(\vec{r}')\right] B(\vec{r}') \cos\theta . d\Omega' \qquad (56)$$

The eigenvalue λ describes the energy fraction re-emitted at each time and is formally equivalent to a mean reflection coefficient: $\lambda = 1 - \overline{\alpha}$.

Breaking the surface in finite elements (boundary elements), it is possible to numerically solve equation (56). Notice however that $B(\vec{r})$ is calculated at different times in both sides of equation (56) to account for propagation: it leads to keep past time in memory - except in the case of steady state regimes - that is, to describe the sound field by a Markov process (Gerlach 1975, Malcurt 1986).

Beside the time memory, the main drawback of wall diffusion is that it does not explain the transition from specular reflection to Lambert law. In fact, all demonstrations of Lambert law are statistical: they assume the sound energy to reach the walls from all directions with the same intensity. Therefore, there is no wonder that the same energy leaves the wall in all directions with the same intensity. Lambert law cannot explains how diffusion gradually sets in a sound field. Notice that wall diffusion is sometime called radiosity.

1.4.5 Mathematical diffusion

Before concluding this section, we wish to compare the assumptions of diffuse sound fields with those of mathematical diffusion which governs the macroscopic propagation of heat. At microscopic level, molecules collide as they move, leading to a random movement call Brownian movement. Whereas molecules collide with each other, sound particle collide with walls: we therefore need to consider the multiple images of the room obtained by mirroring it on all its wall to push the analogy further. As said in Section 1.2.5, the different images of the room do no exactly overlap in the general case, and the network built up by the walls covers the whole space eventually. In this limit situation, mathematical diffusion could make sense in room acoustics.

Mathematical diffusion is described by a behaviour law such as:

$$\vec{I} = w\vec{c} + \delta\vec{\nabla}w \qquad (57)$$

which lead to a diffusion equation when combined with the local energy balance (43):

$$\partial_t w - \vec{c}.\vec{\nabla}w - \delta\Delta w = \Pi(\vec{r}_S, t_S) \qquad (58)$$

This equation admits an analytical solution for an impulsive point-like source located at origin:

$$w(r,t) = \frac{1}{(4\pi\delta t)^{1/2}} exp\left\{-(r-ct)^2 / 4\delta t\right\} \qquad (59)$$

As time goes, the spatial extension of the solution, measured by $\sigma = 2\sqrt{\delta t}$ increases. After sufficient time, the solution covers a volume larger than the room: diffusion is then complete.

However, mathematical diffusion has never been applied to room acoustics yet, probably because of the difficulty to define the diffusion coefficient δ. Nevertheless, it is easy to see that, for c = 0 and δ very large, mathematical diffusion leads to results equivalent to the diffuse field approximation: energy instantaneously diffuses in the whole room, leading to a uniform energy density w in the room in first approximation. Simple calculations leads to the local intensity flows through the walls, and to Sabine's equation when introducing absorption on the walls. As for the diffusion equation itself, it does not introduce any absorption within the room

2. Recent developments in reverberation theory

Recent developments in reverberation theory (Polack 1992, Mortessagne et al. 1992 and 1993, Mortessaone 1994) are all based on billiard theory, that is, on the uniform rectilinear movement of a point in a bounded space with specular reflections on the walls (see Section 1.3.1). The whole Section heavily borrows from Polack (1992).

2.1 Dynamical systems and billiards

Any dynamical system is defined by three elements (Gallavotti 1976):

* a phase space $M = VxS^2$, where V is the volume of the billiard and S^2 the unit three-dimensional sphere, describing the position r as well as the direction, represented by a solid angle $\Omega \in S^2$, taken by the point at any time.

* a group of automorphisms S_t in M, functions of a parameter t, defining the trajectories in the phase space. For billiards, t is the time, and the transformation St is obtained by following the running point initially at (r,Ω) along its uniform rectilinear movement and specular reflections on boundaries until it reaches a new position (r',Ω') at time t. Exchanging initial and final positions while inverting direction, that is, while reversing time, obviously builds the reverse transformation $S_t^{-1}=s_{t-t}$. It is thus straightforward to show that:

$$S_{t+s} = S_t S_s \qquad S_0 = Id\,, \qquad \forall s,\quad t \in R \qquad (60)$$

Thus the transformations S_t build a group.

* a measure μ, defined on the phase space M, and invariant by the transformations S_t, that is, for all μ-measurable subset A of M:

$$\mu(S_t A) = \mu(A) \tag{61}$$

Obviously, the usual Lebesgue's measure on M:

$$d\mu = \frac{dr\, d\Omega}{4\pi V} \tag{62}$$

where 4π is the measure of S^2, is invariant by the transformation S_t (Gallavotti 1976).

As can be seen from the previous definition, billiard theory neglects the interaction between rays: it therefore neglects caustics and diffraction, just as geometrical acoustics, and can only give a high frequency approximation of room acoustics. However, Mortessagne (1994) has shown that the semiclassical approximation extends the results of billiard theory toward the low frequencies.

The best known billiards are the rectangular billiards where almost all trajectories reach almost all positions, but only take 4 different directions in two dimensions (Figure 14), that is, 8 directions in three dimensions. Other shapes have also been investigated, such as polygonal smooth convex billiards, and even concave billiards, with special attention given to their statistical properties.

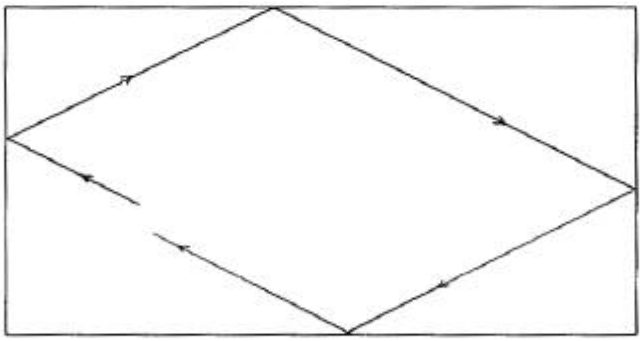

Figure 14: A rectangular billiard

2.2. Statistical properties of billiards.

The statistical properties of billiards make it possible to give an answer to the question: where is the ray located in phase space, that is, both in position and direction, after a given lapse of time ? The first statistical property, ergodicity, considers only one trajectory: along almost any trajectory of an ergodic billiard, the running point spends equal time in the vicinity of each position and each direction (Joyce 1975). Mathematically, it expresses that phase space average is equal to time average for all measurable functions (Sinai 1976, Gallavotti 1976). Let f(x) be the time average of a function f, taken along the trajectory

issued from point x=(r,Q) of the phase space M, and f* the (phase) space average of f, respectively defined by:

$$\overline{f(x)} = \lim_{T \to +\infty} \frac{1}{T} \int_0^T f(S_t x)\, dt\,, \qquad f^* = \int_M f(x)\, d\mu(x) \tag{63}$$

then ergodicity means:

$$\overline{f(x)} = f^* \tag{64}$$

for almost all points x of M. In other words, the probability to reach any phase space point is the same.

A stronger statistical property, mixing, involves two different observation times along a group of initially adjacent trajectories, and can therefore be considered as a correlation property: if we wait long enough between the two observations - strictly speaking, an infinitely long time - two initially adjacent trajectories separate completely and spread over the whole billiard (Joyce 1975). Trajectories can thereafter be considered as statistically independent, and no one knows any longer the position or the direction of the running point. Mathematically for all pairs of measurable functions (f,g):

$$\lim_{T \to +\infty} \frac{1}{T} \int_M f(S_t x) g(x)\, d\mu = \int_M f(x)\, d\mu \int_M g(x)\, d\mu \tag{65}$$

Mixing billiards constitute therefore a subset of ergodic billiards. Though more restrictive than ergodicity, mixing is more fruitful: it makes it possible to define a mixing time as the time after which mixing has occurred. Strictly speaking, this time is infinite, as shown by definition (65), but can be rendered finite within a given tolerance margin. Notice that this definition of mixing time supersedes the one given in Section 1.2.5.

Billiards can also be characterized by their entropy. Directly linked to ergodicity, this quantity can be shown to be related to the logarithmic rate of divergence of trajectories (Benettin & Strelcyn 1978): the Lyapunov characteristic number. Entropy, therefore, involves at least two trajectories. The practical importance of entropy arises from the fact that only mixing billiards have strictly positive entropies (Arnold & Avez 1967) and Lyapunov characteristic numbers (Benettin & Strelcyn 1978). On the other hand, non-ergodic billiards have Lyapunov characteristic numbers and entropies equal to zero. No simple characterisation exists for non-mixing but ergodic billiards.

Since intensity variation along a ray is inverse proportional to the cross-section of a tube built around the ray (see Section 1.3.2), an exponential divergence of rays leads to an exponential decay of energy along any ray. In order to conserve energy in the room, the number of arrivals must increase exponentially with time: this is strongly reminiscent of the diffracted rays of Section 1.3.4.

2.3 Energy decay function and diffusion

In order to build the energy decay function, we first need to chose a source. In mathematical terms this amount to choosing a certain function s(x) defined on the phase space M. Hence, not only the position of the source in the room has to be defined, but also its directivity. The latter is particularly relevant since all physical sources do indeed radiate differently in different directions. The same applies to the receiver, which occupies a certain volume in the room as well as possesses a direction dependent sensitivity: it can also be described by a function r(y) defined on the phase space.

Each of the pulses emitted by the source s(x) at time t=0 travels through the room along the rays $S_t x$. On the way, they hit the walls where they are reflected. Now, in real rooms, pulses loose some energy when they hit a wall, that is, only a portion $R \leq 1$ is reflected. Assuming the reflection coefficient R to be the same on all the walls, the energy carried by each ray issued from point x in the phase space at time t=0, is equal to $R^{n(t)}(x)$ where n(t) is the number of reflections undergone by the ray during its travel time t. On the way, the rays may also cross the receiver, which happens each time $r(S_t x)$ is not zero. In other words, the energy received by the receiver at any time, that is, the energy decay function for any specific choice of source and receiver, is given by:

$$w(t) = \int_M R^{n(t)}(x)\, s(x)\, r(S_t x)\, d\mu(x) \qquad (66)$$

In a mixing room, integral (66) can be splitted according to equation (65), provided we wait longer than the mixing time T. Thus, equation (66) becomes:

$$w(t) = \int_M R^{n(t)}(x)\, s(x)\, d\mu(x) \cdot \int_M r(x)\, d\mu(x), \qquad t > T \qquad (67)$$

and the energy decay function becomes independent of the receiver position and directionality, as long as it occupies the same phase volume. In other words, energy becomes uniformly distributed in the phase space, that is, both in position and direction, after the mixing time has elapsed. This property of mixing room is strongly reminiscent of the diffuse field approximation of Section 1.4.2, but does not suffer of the same inconsistency when absorption is present. Therefore, we propose to replace the traditional definition of diffusion by mixing, which has the advantage of being a purely geometrical property of a room, independent of wall absorption.

2.4 The distribution of reflections as key to the reverberation process

In the previous Section, application of mixing to the energy decay led to a definition independent of the receiver position or directivity (equation 67). Exchanging receiver and source roles by reversing time, mixing leads in a similar fashion to an energy decay function independent of source position or directivity:

$$w(t) = \int_M R^{n(-t)}(x) r(x)\, d\mu(x) \cdot \int_M s(x)\, d\mu(x) \qquad (68)$$

Obviously, these two properties imply the independence of the energy decay from both source and receiver positions and directivities. Therefore, source and receiver terms can be dropped in equation (68), leading to:

$$w(t) = \int_M R^{n(t)}(x)\, d\mu(x) \qquad (69)$$

Now, mixing rooms also are ergodic. The phase space average in equation (69) is therefore equal to a time average of $R^{n(T)}(x)$ obtained by considering the source x as successively taking all (phase) points located along one trajectory. Thus, the energy decay in the room can be written:

$$w(t) = < R^{n(t)} > = \lim_{T\to\infty} \frac{1}{T} \int_0^T R^{n(t)}(S_s x)\, ds \qquad (70)$$

here $S_S x$ is the trajectory issued from any point $x \in M$.

Mixing further ensures that sound energy decays need only be computed over the mixing time: independence of events further apart than mixing time ensures an exponential decay. For example, if t=mT, where T is the mixing time, it can be shown by recursion - using $f(x)=g(x)=R^{n(T)}(x)$ in equation (65) - that:

$$\begin{aligned} < R^{n(t)} > = < R^{n(mT)} > &= \left[< R^{n(T)} > \right]^m = (e^{-aT})^m \\ &= e^{-amT} = e^{-at} \end{aligned} \qquad (71)$$

where $a = - (1/T) \ln[<R^{n(T)}>]$. Hence, mixing is sufficient to ensure an exponential decay, that is, mixing is sufficient to define a reverberation time, independent of source position.

In order to evaluate the reverberation time, it is sufficient to evaluate the mean value taken along one ray by the function $f(x)= R^{n(T)}(x)$, where T is the mixing time. In practice, we need only consider several time intervals equal to the mixing time and evaluate the mean value taken by f(x) on all these intervals. Alternatively, we can evaluate the number of reflections undergone by the ray during each time interval and evaluate the empirical distribution for the number of reflections during the mixing time. If we consider many intervals, this empirical distribution approximates the true probability distribution $p_n(T)$ for the number of reflections during the mixing time T, and the mean value taken by f(x) is given by:

$$< f(x) > = \sum_{n=0}^{\infty} f(x)\, p_n(T) = \sum_{n=0}^{\infty} R^n\, p_n(T) \qquad (72)$$

Now, this distribution is not known, except in the case of instant mixing where it reduces to Poisson distribution and leads to Sabine's reverberation time formula (35). In the general case, the independence of events further apart than the mixing time must be called upon to show that the number of reflections along one ray builds up an additive process with independent increments (see Polack 1992), leading to the general form for the energy decay function:

$$w(t,R) = e^{\Psi(t,\ln|R|)} \cong e^{t\left[\sum_{k=1}^{\infty}\left[R^k-1\right]\sigma_k\right]} \qquad (73)$$

with $\sigma_k \in \leq 0$ and $S\sigma_k < \infty$, and to a generalized Sabine reverberation time:

$$RT = \frac{13.8}{\left[\sum_{k=1}^{\infty}\left[R^k-1\right]\sigma_k\right]} \qquad (74)$$

However, this reverberation time has not been confronted to experiments yet, and must be taken with a grain of salt.

2.5 Path fluctuations and renormalization of decay rate

Instead of evaluating the distribution of reflections, Mortessagne et al. (1992, 1993) and Mortessagne (1994) have focus on path fluctuations, and have numerically simulated reverberation in two-dimensional billiards. They show that Norris-Eyring's reverberation time formula:

$$T_{NE} = \frac{0.16}{S|\ln R|} \qquad (75)$$

must he renormalized into:

$$T_{fluc} = \frac{13.8}{4Vc}\left[\frac{\sigma^2}{\sqrt{1-2(\sigma S/4V)^2 \ln R} - 1}\right] \approx T_{NE}\left[1+\frac{1}{2}(\sigma S/4V)^2|\ln R|\right] \qquad (76)$$

to the third order in ($\sigma Sc/V$), where σ is linked to the standard deviation of path fluctuations. More precisely, the total length L_n of the ray after n reflections is the sum of n successive free-path lengths $\ell_1 + \ell_2 + \ldots + \ell_n$ considered as correlated random variables. Then obviously, L_n fluctuates around its average $\langle L_n \rangle = n\langle \ell \rangle$ where $\langle \_ \rangle$ is the mean free-path equal to (4V/S) in any room. Then σ is given by:

$$\sigma^2 = \lim_{n \to \infty} \sum^2(n)/n \qquad (77)$$

where S(n) is the standard deviation of Ln. Mortessagne et al. (1992, 1993) have numerically checked equation (76): the experimental reverberation time plotted in Figure 15, with arbitrary units, agrees better with equation (76) - upper curve - than with Norris-Eyring's formula (75) - lower curve.

Using the data from Mortessagne et al. (1992, 1993), it is possible to evaluate the σ_k of equations (73) and (74), however only in the case where only one order k is retained. It turns out that the reverberation time, given by equation (74) is not very sensitive to the order k, but that data do not fit with integer values of k: the optimal k is slightly greater than 1/2 (k=0.576 and σ_k=0.795), and formula (76) agrees within 4% with the results plotted in Figure 15.

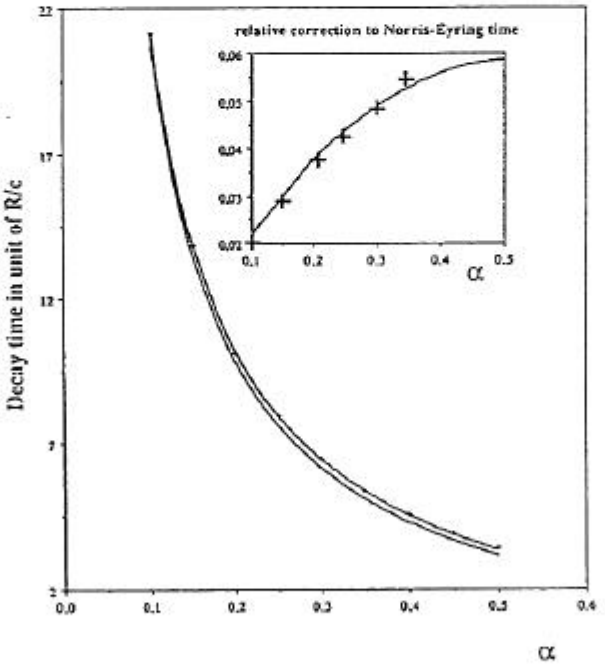

Figure 15: Decay rate renormalisation in a billiard
upper curve: equation(76);lower curve: equation(75);
+ are experimental data (from Mortessagne et al. 1993)

However, better agreement is obtained if k is fixed to 1/2, introducing a zeroth order m in |lnR| in the denominator of equation (74) (m=0.0608 and $\sigma_{1/2}$ = 0.795): the error reduces to 1.5%.

Mortessagne et al. (1993) have also investigated the effect of localised absorption: an exponential decay is no longer achieved, but the decay is dominated by the trajectories trapped between the two parallel walls of their billiard (flutter echo), as seen in Figure 16.

2.6 Non-ergodic billiards

The rectangular billiard of Figure 14 plainly is an example of non-ergodic billiards since each trajectory takes only 4 different directions. Similarly, a rectangular room is non-ergodic. Since rectangular rooms are the constitutive elements of buildings, they deserve special attention.

In a rectangular room, only ray directions remain well-defined. The position of the ray, on the other hand, is uniformly distributed in the room. As a consequence, only a few source and

receiver positions are necessary to assess the energy decay curve in the room, provided they are as omnidirectional as possible. Nevertheless, exponential decay is never obtained, but energy decays at a different rate for different initial directions of the rays, independently of the source position. In fact, each decay rate defines in the phase space a subset containing all points with smaller decay rates: it is obvious that these subsets are included in each other, like Russian dolls. Thus, when observation times increase, the subsets contributing mostly to the energy decays shrink, the instantaneous decay rates decrease, and the instantaneous reverberation times increase. The corresponding energy decay curve is therefore curved convexly upward, as observed in Kuttruff (1973), in a way reminiscent of Figure 16 (however obtained in a mixing billiard).

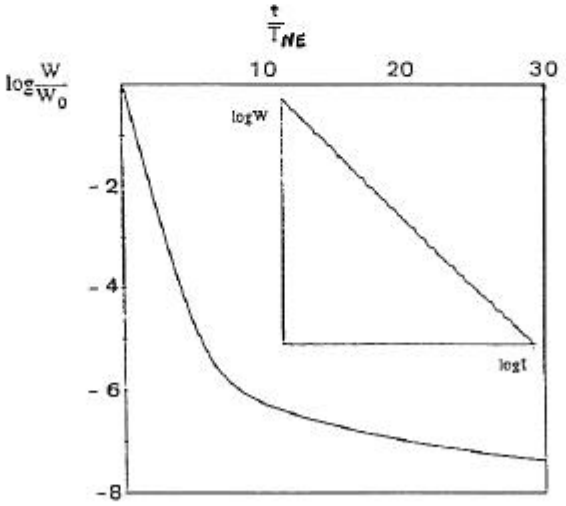

Figure 16: The effect of localised absorption (from Mortessagne et al. 1993)

It is therefore grossly erroneous to generalise results obtained with rectangular rooms. For example, the density of arrivals derived in Section 1.2.5 for rectangular rooms cannot be

extended to other shapes: instead, the energy conservation in dynamical systems must be called upon to evaluate this density, as was briefly mentioned in Section 2.2.

3. Conclusion: The contribution of theoretical room acoustics

This survey of theoretical room acoustics has brought us to the frontier of present knowledge in room acoustics. We have seen how modal analysis must give way to statistical analysis as soon as the number of modes is large, and that this statistical analysis, though well adapted to the description of a steady state reverberation field, fails to explain the gradual onset of reverberation. We had to look instead toward geometrical acoustics, which in its billiard variant of Section 2 leads to mixing rooms where the sound field gradually becomes statistical. On the other hand, rectangular room are not ergodic, and all generalisation of results obtained in such rooms must therefore be taken with caution.

As regards energy analysis, we have stressed the limitations of the diffuse field approximation introduced by Sabine, and have introduced instead the concept of mixing, a geometrical property independent of absorption. With the help of mixing, a consistent theory of reverberation could be developed, generalizing Sabine's theory whose practical validity is thus emphasised.

Throughout this survey, two different descriptions of reflections on the walls of a room have been used: for modal analysis, we used the specific normal admittance; and for both geometrical acoustics and energy analysis, reflection coefficients. Of course, the two descriptions are equivalent, but both are restricted to locally reacting walls, therefore excluding membrane absorbers, widely used in practice. On the other hand, the normal admittance leads to different reflection coefficients for different incidence: this behaviour can be generalized by normal admittance defined for plane waves only and depending on the direction of incidence, as discussed by Morse & Bolt (1944). Such a behaviour greatly complicates modal analysis, but already is included into geometrical acoustics.

In practice, this survey concludes to the superiority of geometrical acoustics as compared to the other approaches, provided its ergodic properties are taken into account. This superiority is confirmed by the fact that only ray-tracing algorithms including statistical treatments of the higher order reflections have reached a point of maturity such as they can be used for reliable predictions in room acoustics. However, these treatments are not yet based on billiard theory. Improvements can therefore be expected along this line, especially with the introduction of semiclassical approximations that allows interferences between rays.

Bibliography

ARNOLD A., AVEZ L. (1967) "Problemes ergodiques de la mécanique classique", Gauthier-Villars, Paris

BALIAN R., BLOCH C. (1970) "Distribution of eigenfrequencies for the wave equation in a finite domain, Part I", Ann. Phys., 60, 401-447

BENEITIN G., STRELCYN J.M. (1978) "Numerical experiments on the free motion of a point mass moving in a plane convex region: stochastic transition and entropy", Phys. Rev. A, 17, 773-785

BOLT R.H., DOAK P.E., WESTERVELT P.J. (1950) "Pulse statistics analysis of room acoustics", J.Acoust.Soc.Am. ,22, 328-340

BOSQUET J. (1967) "La théorie synthétique de la réverbération", Bull. Labo. Acoustique Univ. Liege, 11, 51-67

BRUNEAU M. (1983) "Introduction aux théories de l'acoustique", Université du Maine, Le Mans, France

COURANT R., HILBERT D. (1962) "Methods of Mathematical Physics, Vol. II", Interscience, New York

CREMER L., MULLER H.A., SCHULTZ T.J. (1982) "Principles and Applications of Room Acoustics", Applied Sciences, London

GALLAVOTI G. (1976) "Problèmes ergodiques de la mécanique classique", Ecole Polytechnique Fédérale, Lausanne

GERLACH R.E. (1975) "The reverberation process as Markoff chain: Theory and initial model experirnents", in "Auditorium Acoustics", R.Mackenzie Ed., Applied Sciences, London

JOT J.M. (1992) "Etude et réalisation d'un spatialisateur de sons par modeles physiques et perceptifs", Ph.D. Thesis, Telecom Paris

JOYCE W.D. (1975) "Sabines's reverberation time and ergodic auditoria", J.Acoust.Soc.Am., 58, 643-655

KUHRUFF H. (1973) "Room Acoustics", Applied Sciences, London

LUDWIG D. (1966) "Uniforrn asymptotic expansions at a caustic", Comm. Pure Appl. Math., 29, 215-250

MALCURT C. (1986) "Simulation informatique pour prédire les criteres de qualification acoustique des salles" ,Ph.D. Thesis, Toulouse III, France

MORSE P.M., BOLT R.H. (1944) "Sound waves in rooms", Rev. Mod. Phys., 16, 69-150

MORSE P.M., INGARD K.U. (1968) "Theoretical Acoustics", McGraw Hill, New York

MORTESSAGNE F., LEGRAND O., SORNETTE D. (1992) "Renormalisation of exponentialdecay rates by fluctuations of barrier encounters", Europhys. Lett., 20, 287-293

MORTESSAGNE F., LEGRAND O., SORNETTE D. (1993) "Role of the absorption distribution and generalization of exponential reverberation law in chaotic rooms", J.Acoust.Soc.Am., 94, 154-161

MORTESSAGNE F. (1994) "Dynamique et interférences géométriques dans les billars chaotiques: application a l'acoustique des salles" Ph.D. Thesis, Paris VII

PIERCE A.D. (1981) "Acoustics", McGraw Hill, New York

POLACK J.D. (1988) "La transmission de l'énergie sonore dans les salles", These de Doctorat d'Etat, Le Mans, France

POLACK J.D. (1992) "Modifying chambers to play billiards: the foundations of reverberation theory", Acustica, 76, 257-272

SCHROEDER M.R. (1954a) "Eigenfrequenzstatistik und Anregungsstatistik in Raumen", Acustica, 4, 456-465

SCHROEDER M.R. (1954b) "Die statistischen Parameter der Frequenzkurven von groSen Raumen", Acustica, 4, 594-600

SCHROEDER M.R. (1969) "Frequency-correlation function of frequency responses in rooms", J.Acoust.Soc.Am., 34, 1819-1823

SINAI Ya.G. (1976) "Introduction to ergodic theory", Princeton University Press, Princeton

VAN DEN DUNGEN F.H. (1934) "Acoustique des salles", Institut Belge de Recherches RadioScientifiques, Gauthier-Villars, Paris

VÉR I.L. (1978) "Les champs acoustiques diffus; utilisations judicieuses et abusives", in "Acoustique et vibrations mécaniques dans le batiment et les travaux publics", Coll. UTI-CISCO, Eyrolles, Paris, 32-67